Supporting Information

Fast Translocation of Proteins through Solid State Nanopores

Calin Plesa[1], Stefan W. Kowalczyk[1], Ruben Zinsmeester[1], Alexander Y. Grosberg[2], Yitzhak Rabin[3], Cees Dekker[1]

[1]*Department of Bionanoscience, Kavli Institute of Nanoscience, Delft University of Technology, Lorentzweg 1, 2628 CJ Delft, The Netherlands.*

[2]*Department of Physics and Center for Soft Matter Research, New York University, 4 Washington Place, New York, NY 10003, USA.*

[3]*Department of Physics and Institute for Nanotechnology and Advanced Materials, Bar Ilan University, Ramat Gan 52900, Israel.*

1. Materials and Methods

Solid-state nanopores were fabricated as previously described[1,2]. Nanopores were treated with oxygen plasma for 1 min on both sides, before each measurement. Nanopore containing membranes were mounted into PMMA or PEEK flowcells containing separate aqueous reservoirs on each side of the chip into which Ag/AgCl electrodes were inserted. The flowcell and the amplifier headstage were placed into a Faraday cage. The ionic current was recorded with an Axopatch 200B amplifier with the low-pass filter set to 100 kHz, the resulting signal was digitized at 500 kHz. Unless otherwise noted the traces were digitally filtered with a 10 kHz Gaussian low pass filter. All analysis was done with a set of custom Matlab scripts with GUI front ends, to be described elsewhere. Event rates were calculated by doing an exponential fit to the distribution of times between the leading edges of events. All buffers used 10 mM Tris-HCl with 1mM EDTA at the pH values given in Supplementary Section S2.

Aprotinin (Bovine lung), Ovalbumin (Hen egg), Ferritin (Horse spleen), and Thyroglobulin (Bovine thyroid) were all purchased from GE Healthcare. β-Amylase (Sweet potato) was acquired from Sigma-Aldrich. β-Galactosidase was purchased from Roche Applied Science. hCG (human pregnancy urine) was from Abcam. Streptavidin and Avidin were from Invitrogen. BSA, RecA, and λ-DNA were from New England Biolabs.

2. Experimental translocation data for proteins and dsDNA

The following three tables provide the experimental data used in Figure 2. Experiments without a reference indicate work done as part of this study.

Table S1 - Experimental parameters for protein translocation experiments.

Protein	c	Buffer	pH	r_p	V	J_{obs}	J_{Smo}	J_{obs}/J_{Smo}	*Ref.*
	nM			nm	mV	Hz	Hz		
MBP	1560	1M KCl	7.5	10	50	11	4400	2.5E-3	3
MBP	780	1M KCl	7.5	10	50	8	2200	3.6E-3	3
Aprotinin	1000	1M NaCl	7.5	20	50	0.3097	9850	3.1E-5	
Ovalbumin	1000	1M NaCl	7.5	20	50	0.77	5030	1.5E-4	
β-Amylase	1000	1M NaCl	7.5	20	50	1.69	2760	6.1E-4	
Ferritin	1000	1M NaCl	7.5	20	50	4.13	2440	1.7E-3	
Thyroglobulin	1000	1M NaCl	7.5	20	50	11.95	1810	6.6E-3	
β-Galactosidase	0.92	1M KCl	8	10	50	0.465	1.23	3.8E-1	
β-Galactosidase	2.3	1M KCl	8	10	50	0.704	3.06	2.3E-1	
β-Galactosidase	4.6	1M KCl	8	10	50	0.825	6.13	1.3E-1	
β-Galactosidase	9.2	1M KCl	8	10	50	1.037	12.3	8.5E-2	
β-Galactosidase	23	1M KCl	8	10	50	3.2	30.6	1.0E-1	
β-Galactosidase	46	1M KCl	8	5	50	5.96	30.6	1.9E-1	
β-Galactosidase	46	1M KCl	8	10	50	12.66	61.3	2.1E-1	
β-Galactosidase	46	1M KCl	8	15	50	20.76	91.9	2.3E-1	
β-Galactosidase	46	1M KCl	8	20	50	29.23	123	2.4E-1	
β-Galactosidase	92	1M KCl	8	10	100	24.8	123	2.0E-1	
β-Galactosidase	230	1M KCl	8	10	50	34	306	1.1E-1	
hCG	270	1M KCl	8	10	100	0.34	666	5.1E-4	
hCG	540	1M KCl	8	10	100	1.18	1330	8.9E-4	
hCG	1350	1M KCl	8	5	100	1.6	1670	9.6E-4	
hCG	1350	1M KCl	8	10	100	2.32	3330	7.0E-4	
hCG	1350	1M KCl	8	15	100	3	5000	6.0E-4	
hCG	1350	1M KCl	8	20	100	1.67	6660	2.5E-4	
hCG	2700	1M KCl	8	10	100	2.92	6660	4.4E-4	
Streptavidin	566	1M KCl	8	10	100	2.82	1440	2.0E-3	
Streptavidin	1000	1M KCl	6.6	10	150	2.54	2540	1.0E-3	
Avidin	40	1M KCl	8	10	100	9.84	106	9.3E-2	
Avidin	40	1M KCl	8	10	50	8.48	106	8.0E-2	
Avidin	40	0.05M KCl	8	10	150	40	106	3.8E-1	4
BSA	1500	1M KCl	8	28.5	100	17	9590	1.8E-3	5
BSA	100000	0.4M KCl	7	9	200	111	202000	5.5E-4	6
BSA	4200	0.15M KCl	8	23	50	0.21	21700	9.7E-6	7
Importin-Beta	2900	0.15M KCl	8	23	50	0.27	12200	2.2E-5	7
BSA	400	1M KCl	8	10	100	12.96	897	1.4E-2	
BSA	2000	1M KCl	8	10	50	0.8	4480	1.8E-4	
BSA	2000	1M KCl	8	10	100	1.532	4480	3.4E-4	

Table S2 - Protein information.

Protein	M.W.	Stokes Radius (R_s)	Radius of Gyration (R_g)	PDB ID	Diffusion Constant (D)
	kDa	nm	nm		m^2/s
MBP	42	3.0 [8]	2.2 [9]	1URD	7.45E-11
Aprotinin	6.5	1.64	1.34 [10]	3LDM	1.30E-10
Ovalbumin	45	3.05 [11]	2.7 [12]	1OVA	6.65E-11
β-Amylase	200	4.8 [13]	5.4 [14]	1BTC	3.65E-11
Ferritin	450	6.1 [11]	5.33 [15]	1FHA	3.22E-11
Thyroglobulin	660	8.5 [11]	8.5 [14]		2.39E-11
β-Galactosidase	540	6.86 [16]	4.2 [17]	1BGL	3.52E-11
hCG	36.7	3.3 [18]	3.0 [19]	1HRP	6.52E-11
Streptavidin	53	3.69 [20]	2.5 [21]	2GH7	6.72E-11
Avidin	66	3.37	2.14*	1AVD	7.00E-11
BSA	66.46	3.48 [22]	2.98 [23]	3V03	5.93E-11
Importin-Beta	97		3.97 [24]	2P8Q	4.82E-11

* Determined using HydroPro[25].

With the exception of Avidin, all diffusion constants were determined using the equation of He and Niemeyer[26]

$$D = \frac{6.85\times10^{-8}T}{\eta\sqrt{M^{1/3}\cdot R_g}} \qquad \textbf{(Eq. S1)}$$

where M is the molecular weight of the protein .

Table S3 - dsDNA translocation experimental data.

DNA length	c	Buffer	pH	r_p	V	J_{obs}	J_{Smo}	J_{obs}/J_{Smo}	Ref
bp	nM			nm	mV	Hz	Hz		
2200	3.44	1M KCl	8	10	100	4.4	1.35	3.2697	
2200	7.2	1M KCl	8	4.75	100	7.83	1.34	5.8526	
48514	0.155	1M KCl	8	10	50	0.65	0.0129	50.3402	
48514	0.155	1M KCl	8	10	100	1.03	0.0129	79.7698	
48514	0.3124	1M KCl	8	7.65	120	4.3	0.0199	215.9877	
48514	0.12496	1M KCl	8	10	120	2.1	0.0104	201.7350	
48514	0.06248	1M KCl	8	7	120	0.9	0.00364	247.0225	
15000	1	1M KCl	8.5	3	100	1	0.0449	22.2497	27
48514	0.156	1M KCl	8	7.5*	200	0.22	0.00975	22.5720	28
48514	0.156	1M KCl	8	7.5*	300	0.35	0.00975	35.9100	28

* This study used Al_2O_3 membranes.

Using the worm-like chain model in the limit $l_p << l_c$, the radius of gyration is given by

$$\left\langle R_g \right\rangle = \sqrt{\frac{l_p l_c}{3}} \ . \qquad \textbf{(Eq. S2)}$$

From the Zimm model for linear polymers we have the ratio between the radius of gyration and the hydrodynamic radius as

$$\frac{R_g}{R_H} = \frac{8}{3}\sqrt{\pi} \cong 1.51 \ . \qquad \textbf{(Eq. S3)}$$

Combining these two with the Stokes-Einstein equation

$$D = \frac{k_B T}{6\pi\eta R_H} = \frac{8\sqrt{\pi}k_B T}{18\pi\eta R_g} = \frac{8\sqrt{\pi}k_B T}{18\pi\eta\sqrt{\frac{l_p l_c}{3}}} \ , \qquad \textbf{(Eq. S4)}$$

and using values of 50 nm for the persistence length l_c of dsDNA and $\eta = 8.9 \cdot 10^{-4}\, Pa \cdot s$ for 1M KCl we obtain

$$D = \frac{1.155\times10^{-18}}{R_g} = \frac{8.947\times10^{-15}}{\sqrt{l_c}} \ . \qquad \textbf{(Eq. S5)}$$

Dynamic light scattering measurements were performed on several proteins in the same high salt (1 M) buffer used in the nanopore experiments. The measured radii, shown in Table S4, were consistent with values reported in literature and no evidence of aggregation was observed. Additionally the diffusion constant was calculated from the measured hydrodynamic radii using the Stokes-Einstein equation.

Table S4 – The hydrodynamic radii of several proteins in 1 M salt, as measured by DLS.

Protein	**Hydrodynamic Radius (R_H)**	**Diffusion Constant (D)**
	nm	m^2/s
Ovalbumin	3.25	6.9E-11
β-Amylase	5.05	4.4E-11
Ferritin	6.75	3.3E-11
Thyroglobulin	9.1	2.5E-11
hCG	3.5	7.0E-11

3. Tracking Adsorption by Monitoring Changes in the Event Rate over Time

As a way to asses the amount of adsorption on to the flowcell walls and the SiN membrane, we tracked the event rate as a function of experimental time. Current traces were split up into 3 second segments and the event rate was determined within each of these segments. The positively charged protein Avidin, showed the largest drop over time, with the event rate reduced from 8.5 Hz at the start of the experiment to 3.4 Hz after 1233 seconds, as can be seen in Figure S1b. This was exceptional as there were no significant changes in event rates of other proteins, as shown for example in the Ferritin trace in Figure S1a.

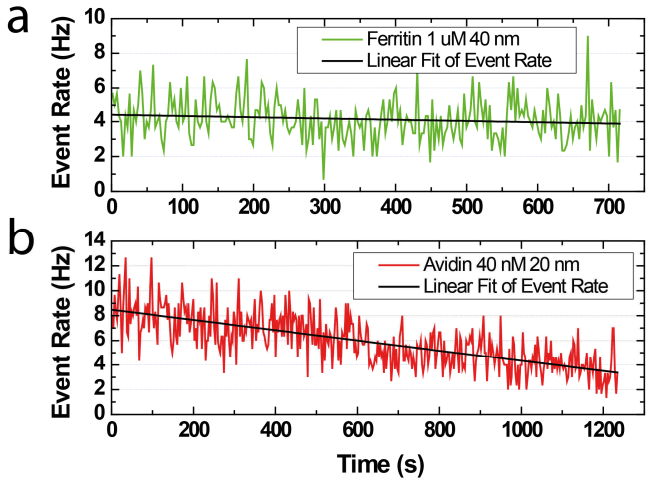

Figure S1. - The event rate as a function of time for (a) Ferritin and (b) Avidin translocation experiments.

4. Protein Charge Measurements

In order to determine the charge of the proteins and calculate their electrophoretic drift velocities, the protein's zeta-potentials were measured using a Malvern Instruments Zetasizer Nano ZS, see Table S5.

Table S5 – Zeta-potential, net valence, and electrophoretic drift velocity.

Protein	**Zeta Potential (ζ_p)**	**Protein Valence**	**Electrophoretic Drift Velocity (v)**
	mV	|z|	m/s
Ovalbumin	-11.7	0.83	2.96E-3
β-Amylase	-12.3	2.05	4.63E-3
Ferritin	-11.4	2.99	5.32E-3
Thyroglobulin	-8.9	4.44	5.67E-3

The zeta potential (ζ_p) is related to the net valence of the protein (z) through the equation[29]

$$z = \frac{\zeta_p \varepsilon R_H \left[1 + \kappa (R_H + R_b\right]}{e\left(1 + \kappa R_b\right)} \quad , \qquad \textbf{(Eq. S6)}$$

where R_b is the average radius of the salt ions (taken to be 0.25 nm), ε is the dielectric constant of the medium, and κ is the Debye–Hückel inverse screening length given by $\kappa = 3.289\sqrt{I}$ in units of nm^{-1}, where I is the ionic strength in M. The values of the net valence were not rounded to nearest integer, due to the possibility that multiple populations with different charged states may exist simultaneously (although β-Amylase and Ferritin valence values clearly correspond to -2e and -3e respectively). This has been observed previously for Avidin[30] and was attributed to heterogeneity caused by various post-translational protein modification processes. The electrophoretic drift velocity is determined using

$$v = \mu_p E = \mu_p \frac{V_p}{h_t} = \frac{e|z|V_p}{6\pi\eta R_H h_t} \quad , \qquad \textbf{(Eq. S7)}$$

where V_p is the portion of the applied voltage that drops over the pore (taking into account the access resistance) and h_t is the effective thickness of the pore.

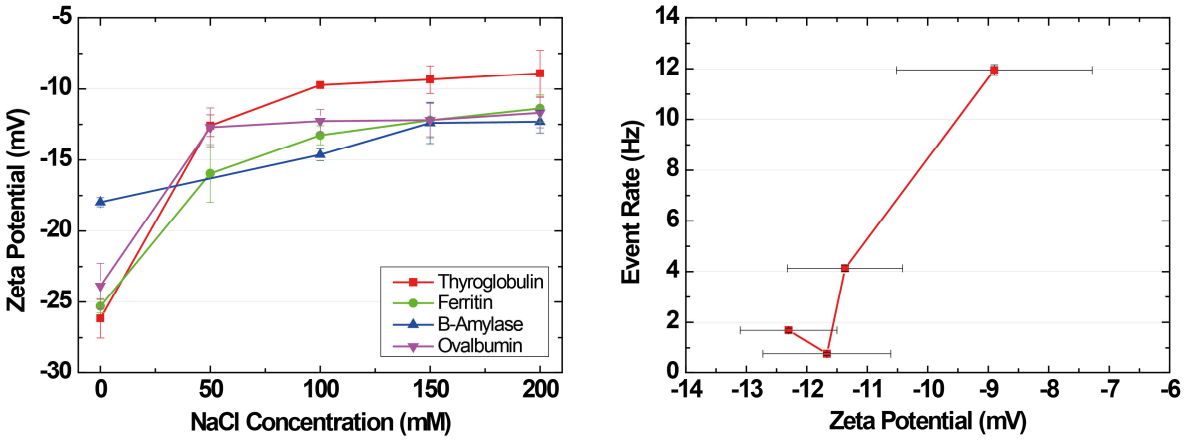

Figure S2. a) Zeta-potential measurements of the proteins used in this experiment as a function of increasing NaCl concentrations with pH 7.5. The largest ionic strength which could be measured was 200mM NaCl. No data could be taken for Aprotinin due to its small size. b) The event rates observed as a function of the protein's zeta-potential.

5. First Passage Time Model

The distributions shown in Figure 3b of the main paper were generated by using the diffusion constants and electrophoretic drift velocities calculated earlier and the cumulative distribution function of the 1D first passage time model as derived by Talaga et al.[31]

$$CDF_{FPTD}(t) = \frac{1}{2} erfc\left(\frac{h_t - vt}{2\sqrt{Dt}}\right) . \qquad \textbf{(Eq. S8)}$$

with an effective membrane thickness of 20 nm. Next the PDF(t) was recovered by inverse transform sampling this cumulative distribution a total of 1,000,000 times. A histogram of this data was generated and normalized. The surface plot shown in Figure 3c was calculated by computing the value of $CDF_{FPTD}(20\ \mu s)$ over the parameter space shown.

6. Filtering Effects

The effects of filtering on the resulting capture rates were investigated. The dependence of the event rate on the filtering frequency for the set of experiments in Figure 4a of the main paper, is shown in Figure S3. While the amplitude of the event rate for each protein varies with the filter frequency, all of the proteins show the same behavior. This means that the trend seen in the event rate the dependence on protein size (Figure 4a) remains the same for all filter settings and with only the absolute values of the event rates changing. The experimentally measured detection level for the 40 nm pores used in these measurements is shown in Figure S4 as a function of the filtering frequency. This shows the minimum amplitude necessary to detect an event. Any events with an amplitude below the threshold (red line) will not be detected.

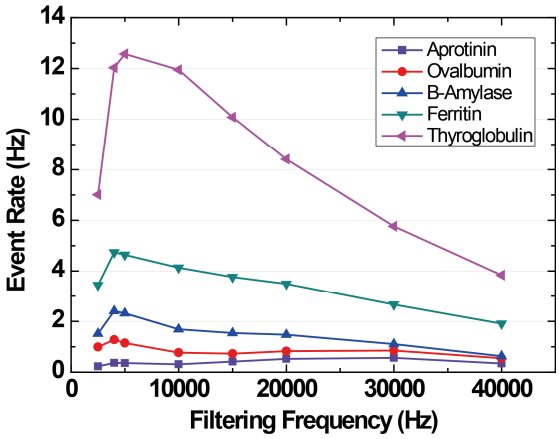

Figure S3. The event rate as a function of the filtering frequency used in the analysis.

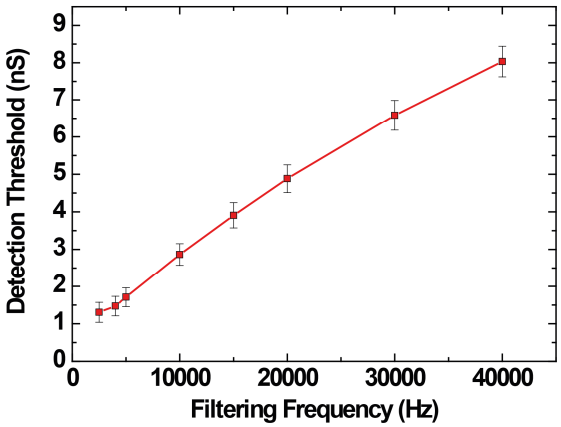

Figure S4. The level of the detection threshold, set as 4.5σ, as a function of the filter frequency as determined experimentally for 40 nm SiN nanopores. This level can be lowered by painting the membrane with a layer of PDMS[32] to reduce the noise.

Furthermore, Figure S5a shows the effect of filtering pulses having an initial amplitude corresponding to the expected blockade for Thyroglobulin (based on its excluded volume). In other words, we generate 4.32 nS pulses ranging in duration from 1 μs to 100 μs. Each of these pulses is then filtered with a 10 kHz Gaussian filter and the resulting filtered pulse amplitude is determined. The intersection of this curve with the threshold line provides the minimum detectable pulse duration (MDPD). This value is determined to be 25 μs for Thyroglobulin. Figure S5b compares all aspects of the experiment from a theoretical perspective. **First**, the black squares show the expected dependence on the diffusion constant, for the five proteins

measured in Figure 4a of the main paper, as predicted by the Smoluchowski rate equation. We see the event rate increase with the diffusion constant. **Secondly**, the red circles represent the prediction of the one-dimensional first-passage time-distribution obtained by multiplying the event rates given by the Smoluchowski rate equation with the probability that an event will translocate within a time larger than 20 μs, the amplifier's temporal limit:

$$J_{FPTD(20\mu s)} = J_{Smo}\left[1 - CDF_{FPTD}(20\mu s)\right] . \qquad \textbf{(Eq. S9)}$$

This also predicts an increase in the event rate as the diffusion constant increases. **Finally**, the blue triangles show the same dependence when the SNR ratio is taken into account. The MDPD was determined for Thyroglobulin and Ferritin and used to define the limit in the first-passage time-distribution:

$$J_{FPTD(MDPD)} = J_{Smo}\left[1 - CDF_{FPTD}(MDPD)\right] . \qquad \textbf{(Eq. S10)}$$

We now see a decrease in the event rate as the diffusion constant increases, which matches the experimentally observed trend (Figure 4a).

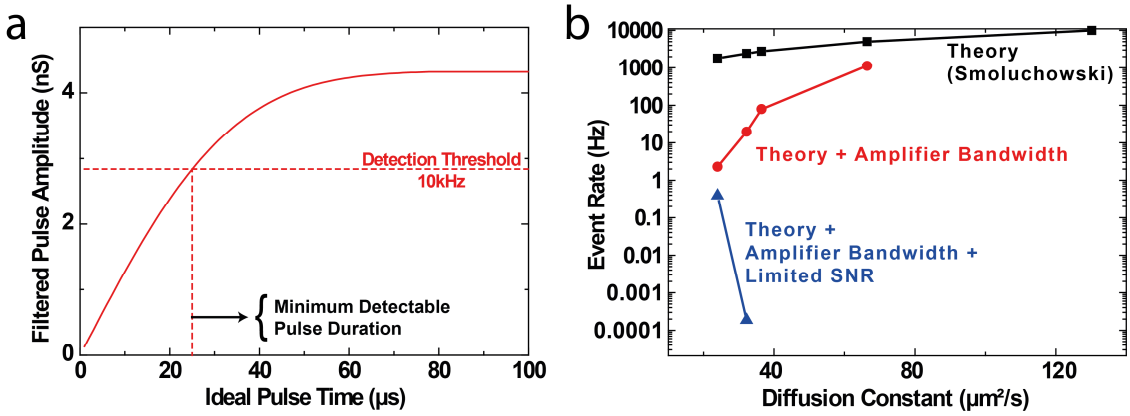

Figure S5. a) Pulses calculated for Thyroglobulin, ΔG = 4.32 nS are Gaussian low-pass filtered to 10 kHz and 5 kHz. The amplitude of the filtered pulse is shown versus pulse duration and compared to the detection threshold. Any event with a pulse duration smaller than the point at which the curve drops below the threshold level will not be detected. b) A comparison of three theoretical models: the Smoluchowski rate equation (black squares), the first-passage time-distribution with amplifier limit of 20 μs (red circles), the first-passage time-distribution with the temporal limit given by the limited SNR of each protein (blue triangles).

For Thyroglobulin the expected amplitude was determined to be 4.32 nS using a shape factor[33] of 1.55 and a partial specific volume[34] of 0.723. For Ferritin the expected amplitude was determined to be 2.86 nS using a shape factor of 1.5 and a partial specific volume[35] of 0.738. In both cases a conductivity of 9.24 S/m was used for 1M NaCl and the expected current drop for each protein was calculated using the same method as Yusko et al.[36]

Table S6 – The data used in Figure S5b.

Protein	***D***	J_{Smo}	***1-CDF(20 μs)***	$J_{FPTD(20\ \mu s)}$	***MDPD***	***1-CDF(MDPD)***	$J_{FPTD(MDPD)}$
	m^2/s	Hz		Hz	μs		Hz
Aprotinin	1.30E-10	4.4					
Ovalbumin	6.65E-11	7.83	0.223546	1123.9			
β-Amylase	3.65E-11	0.65	0.028665	79.1			
Ferritin	3.22E-11	1.03	0.008055	19.6	70	7.76E-08	1.89E-4
Thyroglobulin	2.39E-11	4.3	0.001272	2.3	25	2.17E-04	3.92E-1

7. Noise Floor

The noise floor of our system is defined by the rate of false events due to the noise inherently present in the system. For Gaussian distributed noise, the rate of false events is given by[37]

$$J_{False} = kf_c e^{\left(-\frac{\Phi^2}{2\sigma^2}\right)}, \qquad \textbf{(Eq. S11)}$$

where k is a constant (0.849 flat noise; 1.25 f^2 noise), f_c is the bandwidth (10 kHz), Φ is the detection threshold, and σ is the rms current at this bandwidth. In our experiments the false event rate is expected to lie between 0.34 and 0.5 Hz. A detection threshold of 4.5σ was used in our analysis in order to capture as many low SNR events as possible.

REFERENCES

1. Krapf, D.; Wu, M.-Y.; Smeets, R. M. M.; Zandbergen, H. W.; Dekker, C.; Lemay, S. G. *Nano Letters* **2005,** 6, (1), 105-109.
2. Janssen, X. J. A.; Jonsson, M. P.; Plesa, C.; Soni, G. V.; Dekker, C.; Dekker, N. H. *Nanotechnology* **2012,** 23, (47), 475302.
3. Oukhaled, A.; Cressiot, B.; Bacri, L.; Pastoriza-Gallego, M.; Betton, J.-M.; Bourhis, E.; Jede, R.; Gierak, J.; Auvray, L.; Pelta, J. *ACS nano* **2011,** 5, 3628-38.
4. Firnkes, M.; Pedone, D.; Knezevic, J.; Döblinger, M.; Rant, U. *Nano Letters* **2010,** 10, 2162-7.
5. Han, A.; Schu¨rmann, G.; Mondin, G.; Bitterli, R. A.; Hegelbach, N. G.; de Rooij, N. F.; Staufer, U. *Applied Physics Letters* **2006,** 88, 093901.
6. Fologea, D.; Ledden, B.; McNabb, D. S.; Li, J. *Applied Physics Letters* **2007,** 91, 539011-539013.
7. Kowalczyk, S. W.; Kapinos, L.; Blosser, T. R.; Magalhaes, T.; van Nies, P.; LimRoderick, Y. H.; Dekker, C. *Nat Nano* **2011,** 6, (7), 433-438.
8. Wearsch, P. A.; Nicchitta, C. V. *Biochemistry* **1996,** 35, (51), 16760-16769.
9. Shilton, B. H.; Flocco, M. M.; Nilsson, M.; Mowbray, S. L. *Journal of Molecular Biology* **1996,** 264, (2), 350-363.
10. Appavou, M. S.; Gibrat, G.; Bellissent-Funel, M. C. *Biochimica et Biophysica Acta (BBA) - Proteins & Proteomics* **2006,** 1764, (3), 414-423.
11. Fasman, G. D., *Practical handbook of biochemistry and molecular biology / edited by Gerald D. Fasman*. CRC Press: Boca Raton, Fla. :, 1989.
12. Matsumoto, T.; Inoue, H. *Journal of Colloid and Interface Science* **1993,** 160, (1), 105-109.
13. Miller, L. K.; Tuazon, F. B.; Niu, E.-M.; Sherman, M. R. *Endocrinology* **1981,** 108, (4), 1369-1378.
14. Espeut, J.; Gaussen, A.; Bieling, P.; Morin, V.; Prieto, S.; Fesquet, D.; Surrey, T.; Abrieu, A. *Molecular Cell* **2008,** 29, (5), 637-643.
15. Zipper, P.; Kriechbaum, M.; Durchschlag, H. *J. Phys. IV France* **1993,** 03, (C8), C8-245-C8-248.
16. Potschka, M. *Analytical Biochemistry* **1987,** 162, (1), 47-64.
17. Nurdin, N.; Canaple, L.; Bartkowiak, A.; Desvergne, B.; Hunkeler, D. *Journal of Applied Polymer Science* **2000,** 75, (9), 1165-1175.
18. Bambra, C. S.; Lynch, S. S.; Foxcroft, G. R.; Robinson, G.; Amoroso, E. C. *J Reprod Fertil* **1984,** 71, (1), 227-233.
19. Pilz, I.; Schwarz, E.; Durchschein, W.; Light, A.; Sela, M. *Proceedings of the National Academy of Sciences* **1980,** 77, (1), 117-121.
20. Wu, S.-C.; Wong, S.-L. *Journal of Biological Chemistry* **2005,** 280, (24), 23225-23231.
21. Desruisseaux, C.; Long, D.; Drouin, G.; Slater, G. W. *Macromolecules* **2000,** 34, (1), 44-52.
22. Ikeda, S.; Nishinari, K. *Biomacromolecules* **2000,** 1, (4), 757-763.
23. Anderegg, J. W.; Beeman, W. W.; Shulman, S.; Kaesberg, P. *Journal of the American Chemical Society* **1955,** 77, (11), 2927-2937.
24. Roman, N.; Kirkby, B.; Marfori, M.; Kobe, B.; Forwood, J. K. *Acta Crystallographica Section F* **2009,** 65, (6), 625-628.
25. Ortega, A.; Amorós, D.; García de la Torre, J. *Biophysical journal* **2011,** 101, (4), 892-898.
26. He, L.; Niemeyer, B. *Biotechnology Progress* **2003,** 19, (2), 544-548.
27. Merchant, C. A.; Healy, K.; Wanunu, M.; Ray, V.; Peterman, N.; Bartel, J.; Fischbein, M. D.; Venta, K.; Luo, Z.; Johnson, A. T. C.; Drndic, M. *Nano Letters* **2010,** 10, (8), 2915-2921.
28. Chen, P.; Gu, J.; Brandin, E.; Kim, Y.-R.; Wang, Q.; Branton, D. *Nano Letters* **2004,** 4, (11), 2293-2298.
29. Winzor, D. J. *Analytical Biochemistry* **2004,** 325, (1), 1-20.
30. Han, A.; Creus, M.; Schürmann, G.; Linder, V.; Ward, T. R.; de Rooij, N. F.; Staufer, U. *Analytical Chemistry* **2008,** 80, 4651-8.
31. Talaga, D. S.; Li, J. *Journal of the American Chemical Society* **2009,** 131, 9287-97.
32. Tabard-Cossa, V.; Trivedi, D.; Wiggin, M.; Jetha, N.; Marziali, A. *Nanotechnology* **2007,** 18, (30), 305505.
33. Brumberger, H.; Lipton, J. L.; Dorfman, G.; Nakano, E. *Biochemical Journal* **1974,** 143, (2), 495-6.

34. Derrien, Y.; Michel, R.; Pedersen, K. O.; Roche, J. *Biochimica et Biophysica Acta* **1949,** 3, (0), 436-441.
35. de Haën, C. *Analytical Biochemistry* **1987,** 166, (2), 235-245.
36. Yusko, E. C.; Prangkio, P.; Sept, D.; Rollings, R. C.; Li, J.; Mayer, M. *ACS nano* **2012,** 6, (7), 5909-5919.
37. Sakmann, B.; Neher, E., *Single-Channel Recording*. Springer Science+Business Media: 2009.